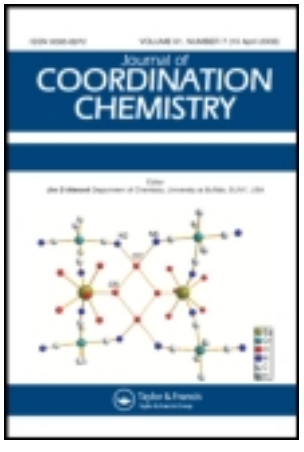

Journal of Coordination Chemistry
Publication details, including instructions for authors and subscription information:
http://www.tandfonline.com/loi/gcoo20

# Preparation and structural, spectroscopic, thermal, and electrochemical characterizations of iron(III) compounds containing dipicolinate and 2-aminopyrimidine or acridine

Masoumeh Tabatabaee [a], Fatemeh Abbasi [a], Boris-Marko Kukovec [b] & Navid Nasirizadeh [c]

[a] Department of Chemistry, Islamic Azad University, Yazd Branch, Yazd, Iran

[b] Laboratory of General and Inorganic Chemistry, Department of Chemistry, Faculty of Science, University of Zagreb, Horvatovac 102a, HR-10000, Zagreb, Croatia

[c] Department of Textile Engineering, Yazd Branch, Islamic Azad University, Yazd, Iran

Published online: 13 May 2011.

To cite this article: Masoumeh Tabatabaee, Fatemeh Abbasi, Boris-Marko Kukovec & Navid Nasirizadeh (2011) Preparation and structural, spectroscopic, thermal, and electrochemical characterizations of iron(III) compounds containing dipicolinate and 2-aminopyrimidine or acridine, Journal of Coordination Chemistry, 64:10, 1718-1728, DOI: 10.1080/00958972.2011.580843

To link to this article: http://dx.doi.org/10.1080/00958972.2011.580843

*Journal of Coordination Chemistry*
Vol. 64, No. 10, 20 May 2011, 1718–1728





# Preparation and structural, spectroscopic, thermal, and electrochemical characterizations of iron(III) compounds containing dipicolinate and 2-aminopyrimidine or acridine

MASOUMEH TABATABAEE*†, FATEMEH ABBASI†, BORIS-MARKO KUKOVEC‡ and NAVID NASIRIZADEH§

†Department of Chemistry, Islamic Azad University, Yazd Branch, Yazd, Iran
‡Laboratory of General and Inorganic Chemistry, Department of Chemistry, Faculty of Science, University of Zagreb, Horvatovac 102a, HR-10000 Zagreb, Croatia
§Department of Textile Engineering, Yazd Branch, Islamic Azad University, Yazd, Iran

(*Received 10 November 2010; in final form 22 March 2011*)

Two new iron(III) compounds, (Hamp)[Fe(pydc)$_2$] · 2H$_2$O (**1**) and (Hacr)[Fe(pydc)$_2$] · 2H$_2$O (**2**) (pydc$^{2-}$ = pyridine-2,6-dicarboxylic acid, amp = 2-aminopyrimidine, acr = acridine), have been hydrothermally synthesized. Both compounds were characterized by spectroscopic methods (IR, UV/Vis), and their molecular and crystal structures were determined by X-ray crystal structure analysis and their thermal stability by thermogravimetric analysis/differential thermal analysis (TGA/DTA) methods. Compound **1** consists of Hamp$^+$ cation and [Fe(pydc)$_2$]$^-$ anion and **2** consists of Hacr$^+$ cation and [Fe(pydc)$_2$]$^-$ anion. Crystallographic characterization revealed an octahedron as a coordination polyhedron for the complex anion in **1** and **2** and the same *O*,*N*,*O*′-chelated coordination mode of pyridine-2,6-dicarboxylate. The crystal structures of **1** and **2** are stabilized by a complicated network of hydrogen bonds between the crystallization water molecules, counter ion, and carboxylates of pydc$^{2-}$. Thermogravimetric (TG) analyses of the two compounds were carried out to examine their thermal stabilities. Cyclic voltammetric response of bare glassy carbon electrode surface in 0.10 mol L$^{-1}$ phosphate buffer containing **1** and **2** at different pH values indicated that they have the same voltammograms at all pH values and the electrochemical behavior of **1** and **2** has not been affected by different ion pairs. The formal potential of the solutions of **1** and **2** at the glassy carbon electrode surface was also pH-dependent with a slope of −57.0 mV/pH unit at 25°C. This shows that the number of electrons and protons involved in the electrode process is equal.

*Keywords*: Crystal structure; Dipicolinate; Iron(III) complex; $\pi$–$\pi$ Interactions; Voltammetry

## 1. Introduction

Polycarboxylates have attracted an interest as potential bridging ligands with a variety of coordination modes in complexes with transition metals and with abundant structural motifs [1–5]. Among polycarboxylic acids, pyridine-2,6-dicarboxylic acid (pydcH$_2$) has attracted much interest in coordination chemistry, because of its low

*Corresponding author. Email: tabatabaee45m@yahoo.com


ISSN 0095-8972 print/ISSN 1029-0389 online 
DOI: 10.1080/00958972.2011.580843

toxicity and amphiphilic nature [6]. Several crystal structures of mononuclear, binuclear, or polynuclear Fe(II) and Fe(III) complexes with $pydcH_2$ and its derivatives have been reported [7]. Dipicolinic acid is a good reagent for the determination of iron [8, 9]. Iron complexes with pyridinedicarboxylic acid derivatives enhance the production of spore photoproducts in bacterial spores upon UV irradiation and activation of dioxygen or hydrogen peroxide in catalytic systems [10]. In continuation of our research on synthesis of the transition metal complexes with polycarboxylate ligands [11, 12], especially pyridine-2,6-dicarboxylate [13–15], we report the synthesis and characterization of two new iron(III) compounds, $(Hamp)[Fe(pydc)_2]\cdot 2H_2O$ (**1**) and $(Hacr)[Fe(pydc)_2]\cdot 2H_2O$ (**2**) ($pydc^{2-}$ = pyridine-2,6-dicarboxylate, $Hamp^+$ = 2-aminopyrimidinium, $Hacr^+$ = acridininum), in this study.



## 2. Experimental

### 2.1. *Materials and instrumentation*

All purchased chemicals were of reagent grade and used without purification. IR spectra were recorded using a FTIR Spectra Bruker Tensor 27 spectrometer (KBr pellets, Nujol mulls, 4000–400 $cm^{-1}$). Absorption spectra were recorded on a Shimadzu Model 160-A UV-VIS spectrophotometer with a 1-cm quartz cell. Thermogravimetric analysis/differential thermal analysis (TGA/DTA) measurements were performed at 10°C $min^{-1}$ from 25°C to 800°C under nitrogen flow of 20 mL $min^{-1}$ on a Rheometrics STA 1500 for **1** and Shimadzu DTG-50H for **2**. Approximately 12 mg of sample was placed in a standard aluminum crucible. All electrochemical experiments were performed with an Autolab potentiostat–galvanostat PGSTAT 30 (Eco chemie, Utrecht, The Netherlands) equipped with GPES 4.9 software, in conjunction with a three-electrode system and a personal computer for data storage and processing. The geometrical area of the bare glassy carbon working electrode (Metrohm, Switzerland) was 0.031 $cm^2$. All the electrochemical experiments were carried out in a conventional three-electrode cell at room temperature. A platinum electrode and a saturated calomel electrode (SCE) were used as the counter and reference electrodes, respectively. All the potentials were reported with respect to this reference electrode. The pH values were measured with a Metrohm model 691 pH/mV meter.

### 2.2. *Preparation of $(Hamp)[Fe(pydc)_2]\cdot 2H_2O$ (1)*

Pyridine-2,6-dicarboxylic acid (0.167 g, 1 mmol) was dissolved in methanol (5 mL) and a solution of NaOH (0.08 g, 2 mmol) in deionized water (10 mL) was added and stirred for 30 min at room temperature. Then, an aqueous solution of $FeCl_3\cdot 6H_2O$ (0.270 g, 1 mmol) and 2-aminopyrimidine (0.095 g, 1 mmol) was added into the above-mentioned solution. Reaction mixture was placed in a Parr-Teflon lined stainless steel vessel, sealed, and heated at 130°C for 8 h. The reaction mixture was gradually cooled to room temperature and the mother liquor was then kept at 4°C until green crystals of **1** suitable for X-ray diffraction were obtained. Yield: 0.225 g (87%, based on dipicolinic acid). IR (KBr) ($\tilde{\upsilon}$, $cm^{-1}$): 3581–3473 (b), 3069 (m), 1679 (s), 1627(s), 1593, 1334 (s), 1263 (m), 1082 (s), 1030 (m), 919 (s), 774 (s), 748 (s), 583 (m), 437 (s).

UV/Vis (aqueous solution) (λ, nm): 216, 262, 478. Anal. Calcd for $C_{18}H_{16}FeN_5O_{10}$: C, 41.7; H, 3.08; N, 13.5%. Found: C, 41.01; H, 3.00; N, 13.39%.

### 2.3. *Preparation of (Hacr)[Fe(pydc)$_2$]·2H$_2$O (2)*

Pyridine-2,6-dicarboxylic acid (0.167 g, 1 mmol) was dissolved in methanol (5 mL) and a solution of NaOH (0.08 g, 2 mmol) in deionized water (10 mL) was added and stirred for 30 min at room temperature. Then an aqueous solution of $FeCl_3 \cdot 6H_2O$ (0.270 g, 1 mmol) and acridine (0.18 g, 1 mmol) was added into the above-mentioned solution. Reaction mixture was placed in a Parr-Teflon lined stainless steel vessel, sealed, and heated at 130°C for 8 h. The reaction mixture was gradually cooled to room temperature. The mother liquor was kept at room temperature until orange red crystals of **2** suitable for X-ray diffraction were obtained. Yield: 0.238 g (79%, based on dipicolinic acid). IR (KBr) ($\tilde{\upsilon}$, $cm^{-1}$): 3514–3406 (b), 3043 (m), 1671 (s), 1627 (s), 1508 (m), 1460 (s), 1363(s), 1315 (s), 1160 (s), 1067 (m), 1030 (m), 919 (s), 770(s), 733 (s), 593 (m), 459 (m). UV/Vis (aqueous solution) (λ, nm): 208, 245, 508. Anal. Calcd for $C_{27}H_{20}FeN_3O_{10}$: C, 53.79; H, 3.32; N, 6.97%. Found: C, 53.73; H, 3.28; N, 6.89%.

### 2.4. *X-ray crystallography*

The data collection for **1** was carried out by a Bruker APEX-II CCD diffractometer, while the data collection for **2** was carried out by an Oxford Diffraction Xcalibur four-circle kappa geometry diffractometer with Xcalibur Sapphire 3 CCD detector by applying the CrysAlis Software system, Version 171.32.29 [16]. Data reduction was done by the same program [16]. Graphite monochromated Mo-Kα (λ = 0.71073 Å) radiation was used in both cases.

X-ray diffraction data have been corrected for Lorentz-polarization factor and scaled for absorption effects by multi-scan. The structure of **1** was solved by direct methods, while the structure of **2** was solved by the Patterson method. Refinement by full-matrix least squares methods based on $F^2$ against all reflections has been performed, including anisotropic displacement parameters for all non-H atoms.

The position of hydrogens belonging to carbon $Csp^2$ was geometrically optimized applying the riding model ($Csp^2$–H, 0.95 Å for **1** and 0.93 Å for **2**; $U_{iso}(H) = 1.2U_{eq}(C)$). Hydrogens belonging to water, to N3 in **1** and **2**, and to the amine of 2-aminopyrimidinium in **1** were found in the difference Fourier maps. The distance between the water oxygen and the corresponding hydrogens was restrained to the average value of 0.84(3) Å in the case of **1** and 0.82(3) Å in the case of **2** using SHELXL-97 DFIX instruction, while the distance between the nitrogens and the corresponding hydrogens was restrained to the average value of 0.88(3) Å in the case of **1** and 0.86(3) Å for **2** using the same instruction. The isotropic $U_{iso}(H)$ values for all hydrogens were fixed at $U_{iso}(H) = 1.2U_{eq}(O)$ for hydrogens belonging to *O* and $U_{iso}(H) = 1.2U_{eq}(N)$ for those belonging to *N*.

Calculations were performed with SHELXS-97 [17], SHELXL-97 [17], and PLATON [18]. The molecular graphics were done with ORTEP-3 [19] and MERCURY (Version 2.3) [20]. The crystal parameters, data collection, and refinement results for both compounds are summarized in table 1.

Table 1. Crystal data and details of the structure determination for **1** and **2**.

| Compound | **1** | **2** |
|---|---|---|
| Formula | $C_{18}H_{16}FeN_5O_{10}$ | $C_{27}H_{20}FeN_3O_{10}$ |
| $M_r$ | 518.21 | 602.31 |
| Temperature (K) | 100(2) | 296(2) |
| Color, habit | Green, block | Orange red, block |
| Crystal system, space group | Monoclinic, $P2_1/c$ | Monoclinic, $P2_1/n$ |
| Unit cell dimensions (Å, °) | | |
| $a$ | 9.4623(10) | 13.296(2) |
| $b$ | 17.991(2) | 10.026(5) |
| $c$ | 11.8823(12) | 20.069(2) |
| $\beta$ | 95.408(2) | 109.009(16) |
| Volume (Å$^3$), $Z$ | 2013.8(4), 4 | 2529.4(13), 4 |
| Calculated density (g cm$^{-3}$) | 1.709 | 1.582 |
| μ (mm$^{-1}$) | 0.820 | 0.664 |
| $F$(000) | 1060 | 1236 |
| Crystal dimensions (mm$^3$) | $0.58 \times 0.30 \times 0.22$ | $0.62 \times 0.52 \times 0.35$ |
| $\theta$ range for data collection (°) | 2.06–34.04 | 3.84–27.00 |
| $h$, $k$, $l$ range | −13:14, −27:28, −18:18 | −16:11, −12:12, −25:25 |
| Scan type | $\omega$, $\varphi$ | $\omega$, $\varphi$ |
| No. measured reflections | 58,146 | 18,910 |
| No. independent reflections ($R_{int}$) | 8205 (0.0313) | 5471 (0.0290) |
| No. observed reflections, $I \geq 2\sigma(I)$ | 6938 | 3220 |
| No. refined parameters | 328 | 385 |
| Goodness of fit on $F^2$, $S$[a] | 1.049 | 0.876 |
| $R$[b], $wR$[c] [$I \geq 2\sigma(I)$] | 0.0289, 0.0732 | 0.0380, 0.0774 |
| $R$, $wR$ [all data] | 0.0384, 0.0777 | 0.0802, 0.0850 |
| Max. and min. electron density (e Å$^{-3}$) | 0.53 and −0.34 | 0.43 and −0.27 |

[a] $S = \Sigma[w(F_o^2 - F_c^2)^2/(N_{obs} - N_{param})]^{1/2}$.
[b] $R = \Sigma||F_o| - |F_c||/\Sigma|F_o|$.
[c] $wR = [\Sigma(F_o^2 - F_c^2)^2/\Sigma w(F_o^2)^2]^{1/2}$.

## 3. Results and discussion

### 3.1. *Preparation of complexes*

Treatment of $FeCl_3 \cdot 6H_2O$ with pyridine-2,6-dicarboxylic acid in the presence of NaOH and 2-aminopyrimidine or acridine in the molar ratio of 1 : 2 : 1 : 1 and under hydrothermal conditions gave **1** or **2**. Compound **1** is green and **2** are orange red blocks; both compounds are stable in air and soluble in water.

### 3.2. *Crystal structures of 1 and 2*

Selected bond lengths and angles are given in table 2. ORTEP-3 views of the molecular structures of **1** and **2** are depicted in figures 1 and 2, respectively. Both compounds consist of an $[Fe(pydc)_2]^-$ and $ampH^+$ (**1**) or $acrH^+$ (**2**) and two uncoordinated water molecules. The iron(III) in **1** and **2** is six-coordinate by two tridentate $pydc^{2-}$ and the geometry of the resulting $FeN_2O_4$ coordination can be described as distorted octahedral. The bond angles around Fe(III) involving *trans* pairs of donor atoms are 151.14(3)–167.21(3)° for **1** and 151.54(6)–169.83(6)° for **2**, deviating from linearity. For *cis* donor atoms this range is 75.09(3)–114.64(3)° for **1** and 75.53(6)–106.53(6)° for **2** (table 2). These values indicate large distortion from ideal octahedral geometry due to the binding of dipicolinate to Fe(III) in tridentate-*O*,*N*,*O*′ fashion in both **1** and **2**. The

Table 2. Selected bond distances (Å) and angles (°) for **1** and **2**.

| | **1** | **2** |
|---|---|---|
| Fe1–N1 | 2.064(1) | 2.049(2) |
| Fe1–N2 | 2.049(1) | 2.065(2) |
| Fe1–O1 | 2.058(1) | 2.031(1) |
| Fe1–O3 | 1.978(1) | 2.000(1) |
| Fe1–O5 | 2.006(1) | 1.987(1) |
| Fe1–O7 | 2.051(1) | 2.042(2) |
| O1–Fe1–N1 | 75.09(3) | 75.93(6) |
| O3–Fe1–N1 | 76.51(3) | 76.33(6) |
| O5–Fe1–N1 | 114.64(3) | 113.84(6) |
| O7–Fe1–N1 | 93.10(3) | 94.61(6) |
| O1–Fe1–N2 | 99.00(3) | 106.53(6) |
| O3–Fe1–N2 | 109.86(3) | 101.46(6) |
| O5–Fe1–N2 | 76.63(3) | 76.08(6) |
| O7–Fe1–N2 | 75.61(3) | 75.53(6) |
| O3–Fe1–O1 | 151.14(3) | 151.99(6) |
| O5–Fe1–O1 | 93.33(3) | 93.83(6) |
| O7–Fe1–O1 | 92.17(3) | 92.20(6) |
| O5–Fe1–O3 | 93.86(3) | 93.80(6) |
| O7–Fe1–O3 | 94.35(3) | 93.81(7) |
| O7–Fe1–O5 | 152.21(3) | 151.54(6) |
| N1–Fe1–N2 | 167.21(3) | 169.83(6) |

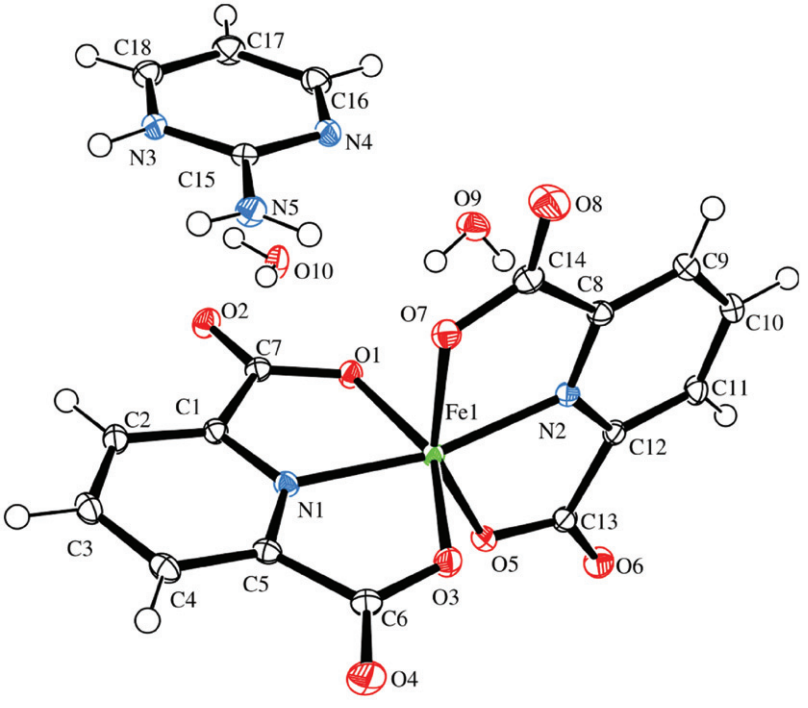


Figure 1. ORTEP-3 drawing of (Hamp)[Fe(pydc)$_2$]·2H$_2$O (**1**) with the atomic numbering scheme of the asymmetric unit. The thermal ellipsoids are drawn at the 50% probability level at 100 K.

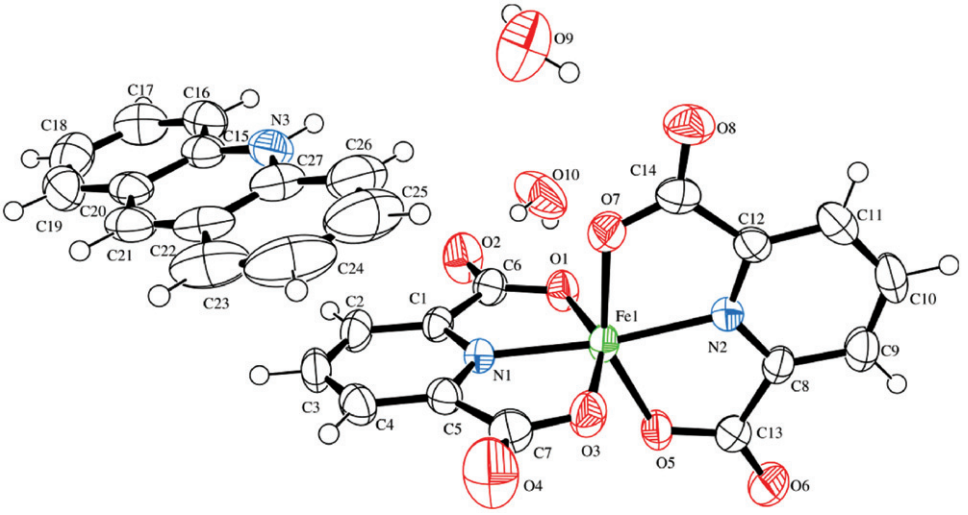


Figure 2. ORTEP-3 drawing of (Hacr)[Fe(pydc)$_2$]·2H$_2$O (**2**) with the atomic numbering scheme of the asymmetric unit. The thermal ellipsoids are drawn at the 50% probability level at 296 K.

Table 3. Hydrogen bond geometry for **1** and **2**.

| D–H···A | *d*(D–H)/Å | *d*(H···A)/Å | *d*(D···A)/Å | ∠(D–H···A)/° | Symmetry code on A |
|---|---|---|---|---|---|
| **1** | | | | | |
| N3–H31···O10 | 0.89(1) | 1.82(1) | 2.677(1) | 164(1) | $x, 1/2-y, -1/2+z$ |
| N5–H51···O4 | 0.83(1) | 2.31(2) | 2.731(1) | 112(1) | $-x, 1-y, -z$ |
| N5–H51···O10 | 0.83(1) | 2.48(2) | 3.133(1) | 137(1) | $x, 1/2-y, -1/2+z$ |
| N5–H52···O7 | 0.85(2) | 2.20(2) | 3.015(1) | 159(1) | $x, y, z$ |
| O9–H91···O1 | 0.84(2) | 2.17(2) | 3.005(1) | 170(2) | $x, y, z$ |
| O9–H92···O2 | 0.86(2) | 2.10(2) | 2.951(1) | 173(2) | $x, 1/2-y, 1/2+z$ |
| O10–H101···O2 | 0.81(2) | 2.05(2) | 2.844(1) | 166(2) | $x, y, z$ |
| O10–H102···O8 | 0.81(2) | 1.90(2) | 2.700(1) | 174(2) | $1-x, -1/2+y, 1/2-z$ |
| **2** | | | | | |
| N3–H31···O10 | 0.87(2) | 1.84(2) | 2.701(4) | 172(2) | $x, y, z$ |
| O9–H91···O2 | 0.82(3) | 2.24(3) | 3.041(3) | 165(3) | $1/2-x, -1/2+y, 1/2-z$ |
| O9–H92···O8 | 0.82(3) | 2.02(3) | 2.832(3) | 170(3) | $x, y, z$ |
| O10–H101···O2 | 0.81(3) | 1.93(3) | 2.747(3) | 179(4) | $1/2-x, -1/2+y, 1/2-z$ |
| O10–H102···O9 | 0.82(2) | 1.84(2) | 2.636(3) | 164(3) | $1/2-x, 1/2+y, 1/2-z$ |

dihedral angles between mean planes of the pyridine rings of pydc$^{2-}$ are 85.57(5)° for **1** and 88.9(1)° for **2**, indicating that pydc$^{2-}$ fragments in both compounds are almost perpendicular to each other. The bond distances Fe–N and Fe–O in **1** and **2** are in accord with values from the literature [7, 21].

Extensive O–H···O and N–H···O hydrogen-bonding interactions (table 3) between N–H of cations, carboxylate of pydc$^{2-}$, and uncoordinated water contribute to the formation of a 3-D structure for **1** (figure 3) and 1-D chain extending along [0 1 0] direction for **2** (figure 4). These chains are further assembled into a 3-D structure. There are also some interactions between chelate rings and the pyrimidine ring in **1** and $\pi$–$\pi$ stacking interactions between pyridine and acridine rings in **2** defined by N1/C1/C2/C3/C4/C5 and C22$^{i}$/C23$^{i}$/C24$^{i}$/C25$^{i}$/C26$^{i}$/C27$^{i}$ [symmetry code $^{i}x, y, z$; centroid–centroid

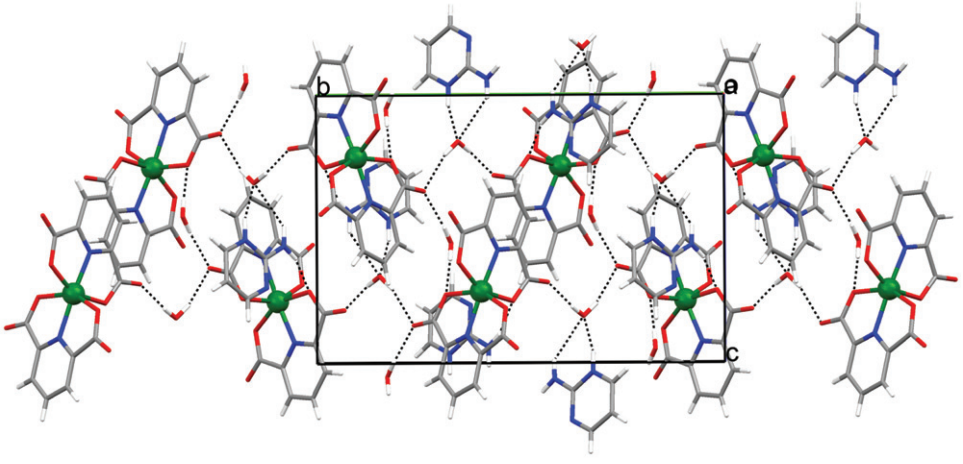


Figure 3. A view of the crystal structure of **1** in the *bc* plane. The cation, complex anion, and water molecules are linked by hydrogen bonds of the O–H···O and N–H···O types (represented by dotted lines) into a 3-D structure.

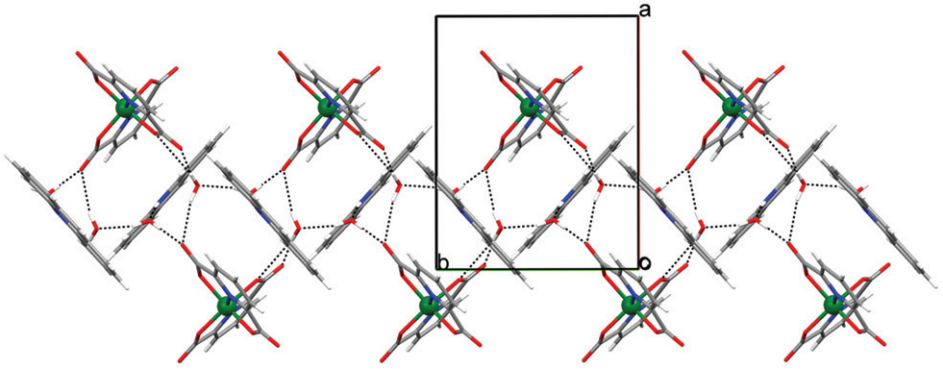


Figure 4. A view of the crystal structure of **2** in the *ab* plane. The cation, complex anion, and water molecules are linked by hydrogen bonds of the O–H···O and N–H···O types (represented by dotted lines) into a 1-D chain along [0 1 0] direction.

distance 3.779(2) Å; the angle between the planes is 10.6(1)°; the perpendicular distance between the planes is 3.531(3) Å; the slippage is 1.856 Å], N2/C8/C9/C10/C11/C12 and $C22^{ii}/C23^{ii}/C24^{ii}/C25^{ii}/C26^{ii}/C27^{ii}$ [symmetry code $^{ii}1/2+x,\ 1/2-y,\ 1/2+z$; centroid–centroid distance is 3.683(2) Å; the angle between the planes is 8.8(1)°; the perpendicular distance between the planes is 3.468(1) Å; the slippage is 1.408 Å], and finally N2/C8/C9/C10/C11/C12 and $N3^{ii}/C15^{ii}/C20^{ii}/C21^{ii}/C22^{ii}/C27^{ii}$ [symmetry code $^{ii}1/2+x,\ 1/2-y,\ 1/2+z$; centroid–centroid distance is 3.671(2) Å; the angle between the planes is 8.4(1)°; the perpendicular distance between the planes is 3.462(1) Å; the slippage is 1.396 Å].

### 3.3. *IR spectra*

Patterns of IR spectra of both compounds show two sets of vibrations due to water and dipicolinate. The carboxylate may coordinate to a metal in unidentate, bidentate, or

bridging modes [22]. In the spectra of **1** and **2**, the band associated with the antisymmetric stretching vibrational mode, $\nu_{as}$ (–$COO^-$), appears at 1679 $cm^{-1}$ (**1**) and 1671 $cm^{-1}$ (**2**) (1700 $cm^{-1}$ in the spectrum of free $pydcH_2$), together with the $\nu_s$ (–$COO^-$) band at 1334 $cm^{-1}$ (**1**) and 1363 $cm^{-1}$ (**2**) (1326 $cm^{-1}$ in the spectrum of free $pydcH_2$). The value of $\Delta(\nu_{as}$ (–$COO^-$)–$\nu_s$ (–$COO^-$)) of 345 and 308 $cm^{-1}$ for **1** and **2** indicate the presence of carboxylate coordinated unidentately to iron(III) [23, 24], in agreement with the crystal structures of **1** and **2**. IR spectra of both complexes show broad strong bands at 3400–3000 $cm^{-1}$, which could be related to the existence of O–H $\cdots$ O hydrogen bonds between water [25]. These bands are coupled to other peaks such as N–H and O–H stretching frequencies and the stretching frequencies corresponding to the aromatic rings which originally fall within this region [26].

### 3.4. *Electronic spectra*

Electronic spectra of aqueous solutions of **1** and **2** display some strong absorptions below 300 nm (216 nm ($\varepsilon = 1.86 \times 10^4\,mol^{-1}\,dm^3\,cm^{-1}$) and 262 nm ($\varepsilon = 6.05 \times 10^3\,mol^{-1}\,dm^3\,cm^{-1}$) (**1**) and 208 nm ($\varepsilon = 3.89 \times 10^5\,mol^{-1}\,dm^3\,cm^{-1}$) and 249 nm ($\varepsilon = 6.40 \times 10^4\,mol^{-1}dm^3\,cm^{-1}$)) (**2**), which are assigned to $\pi \rightarrow \pi$ transition of the aromatic compounds. The spectra of **1** and **2** show absorption bands at 478 nm ($\varepsilon = 8.75 \times 10^1\,mol^{-1}\,dm^3\,cm^{-1}$) and 508 nm ($\varepsilon = 1.87 \times 10^2\,mol^{-1}\,dm^3\,cm^{-1}$), respectively. These bands are due to a strong charge-transfer (CT) band tailing from the UV-region to the visible region [27].

### 3.5. *Thermal analysis (TGA/DTA)*

The TGA curve for **1** shows that the first weight loss from 170°C to 207°C corresponds to the loss of $ampH^+$ (experimental value 18.84% and calculated 18.52%). The second stage occurs from 350°C to 650°C with weight loss corresponding to total decomposition of the compound. The TG curve shows 69.20% weight loss at 726°C, indicating the complete removal of organic part of the compound. The main product was $Fe_2O_3$ with a residual value of 30.80% (theoretical residual value, 30.87%). The thermal decomposition of **2** is similar to that of **1**, with the first and second weight losses from 250°C to 275°C and 305°C to 410°C, respectively. Further decomposition of **2** began at 520°C and finished at 675°C.

### 3.6. *Electrochemical behavior*

Cyclic voltammetric response of bare glassy carbon electrode surface in 0.10 mol $L^{-1}$ phosphate buffer solutions containing **1** and **2** at different pH values has been investigated. The two compounds have the same voltammograms at all pH values investigated. These cyclic voltammograms indicate that the different ion pairs of **1** and **2** do not have any effect on their electrochemical behavior. The voltammograms of bare glassy carbon electrode surface in 0.10 mol $L^{-1}$ phosphate buffer solutions containing 0.3 mmol $L^{-1}$ of **2** in the pH range of 2.0–4.5 are shown in figure 5. The anodic and cathodic peak potentials shift to negative potential values with increasing pH. The formal potential, $E^{0'} = (E_{pa} + E_{pc})/2$, of **1** and **2** solutions at the glassy carbon electrode

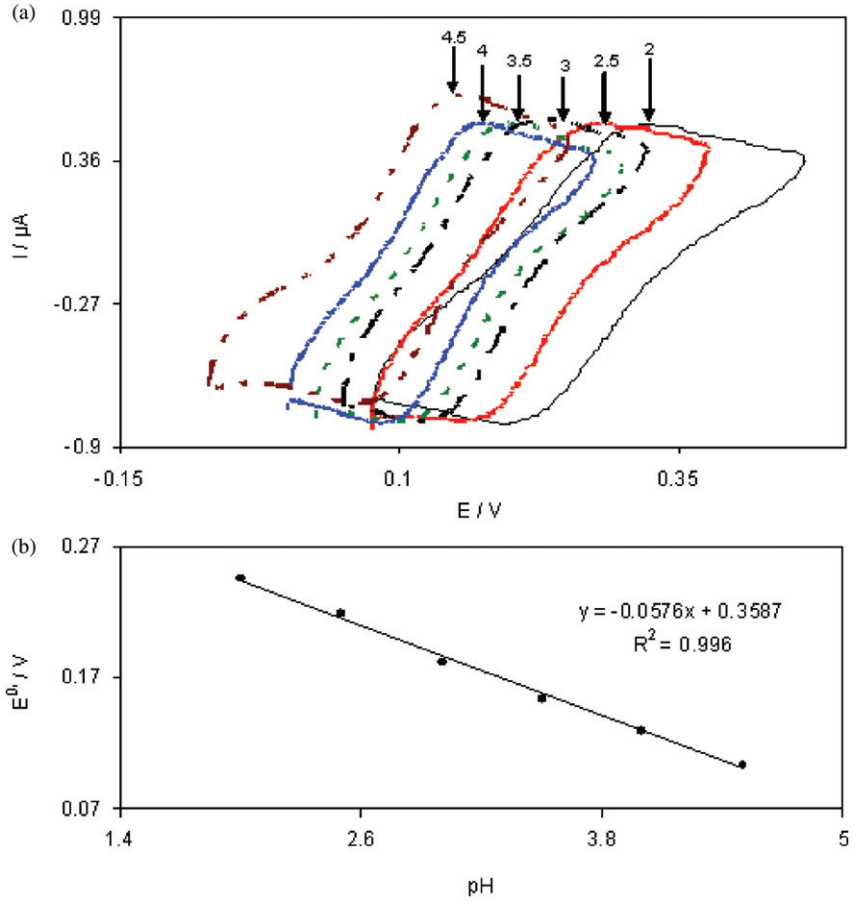


Figure 5. (a) Cyclic voltammograms of a glassy carbon electrode (at 100 mV $s^{-1}$) in 0.10 mol $L^{-1}$ phosphate buffer solution containing 0.3 mmol $L^{-1}$ of **2** at different pH values: 2.0, 2.5, 3.0, 3.5, 4.0, and 4.5; and (b) the plot of the formal potential, $E^{0\prime}$, *vs.* pH.

surface was pH-dependent with a slope of −57.0 mV/pH unit at 25°C. The linear relationship of the $E^{0\prime}$ *versus* pH was used to determine the number of protons (m) transferred for a given oxidation through the Nernst equation [28]. The slope of $E^{0\prime}$ *versus* pH is:

$$\text{Slope} = -\text{mRT/nF}.$$

The Nernstian slope of −0.059 V/pH unit at 25°C indicates that the number of electrons and protons involved in the electrode process is equal. Therefore, the redox reactions in aqueous solutions of **1** and **2** occur with participation of one electron and one proton and the following equation has been proposed:

$$[\text{Fe(pydc)}_2]^- + H^+ + e^- \leftrightarrow [\text{Fe(pydcH)(pydc)}]^-.$$

Also, from the intercept of figure 5(b) inset, the standard formal potential of **2** was obtained, 0.358 mV. The reduction potential of Fe(III) into Fe(II) in a complex depends

on its stability. Indeed, with the increase in complex stability less positive potential is needed for the reduction of cation. Since the reduction potential of Fe(III) in $[Fe(CN)_6]^{3-}$ (0.12 V) [29] is less than that of Fe(III) in **2** (0.358 V), it can be concluded that $[Fe(CN)_6]^{3-}$ is more stable than $[Fe(pydc)_2]^{-}$.

## Supplementary material

CCDC 779832 for **1** and 779833 for **2** contain the supplementary crystallographic data for this article. These data can be obtained free of charge *via* www.ccdc.cam.ac.uk/conts/retrieving.html [or from the Cambridge Crystallographic Data Centre (CCDC), 12 Union Road, Cambridge CB2 1EZ, UK; Fax: +44 1223 336033; Email: deposit@ccdc.cam.ac.uk]. Structure factor table is available from the authors.



## Acknowledgments

This research was supported by the Ministry of Science, Education and Sports of the Republic of Croatia (Grant no. 119-1193079-1332), and Islamic Azad University, Yazd Branch.

## References

[1] Y.H. Wen, J.K. Cheng, Y.L. Feng, J. Zhang, Z.J. Li, Y.G. Yao. *Inorg. Chim. Acta*, **358**, 3347 (2005).
[2] A. Thirumurugan, S. Natarajan. *Eur. J. Inorg. Chem.*, 762 (2004).
[3] J.C. Yao, W. Huang, B. Li, S. Gou, Y. Xu. *Inorg. Chem. Commun.*, **5**, 711 (2002).
[4] X.M. Zhang, M.L. Tong, M.L. Gong, X.M. Chen. *Eur. J. Inorg. Chem.*, 138 (2003).
[5] H. Li, C.E. Davis, F.L. Croy, D.G. Kelley, O.M. Yaghi. *J. Am. Chem. Soc.*, **120**, 2186 (1998).
[6] E. Norkus, I. Stalnionienė. *Chemija (Vilnius)*, **13**, 194 (2002).
[7] K.A. Abboud, C. Xu, R.S. Drago. *Acta Crystallogr.*, **C54**, 1270 (1998).
[8] Y. Kanay. *Analyst*, **115**, 809 (1990).
[9] I. Morimoto, S. Tanaka. *Anal. Chem.*, **35**, 141 (1963).
[10] B. Setlow, P. Setlow. *Appl. Environ. Microbiol.*, **59**, 640 (1993).
[11] M. Tabatabaee, M. Ghassemzadeh, F. Rezaie, H.R. Khavasi, M.M. Amini. *Acta Crystallogr.*, **E62**, m2784 (2006).
[12] M. Tabatabaee, M.A. Sharif, F. Vakili, S. Saheli. *J. Rare Earths*, **27**, 356 (2009).
[13] M. Tabatabaee, H. Aghabozorg, J. Attar Gharamaleki, M.A. Sharif. *Acta Crystallogr.*, **E65**, m473 (2009).
[14] M. Tabatabaee, R. Mohamadinasab, K. Ghaini, H.R. Khavasi. *Bull. Chem. Soc. Ethiop.*, **24**, 401 (2010).
[15] M. Tabatabaee. *Acta Crystallogr.*, **E66**, m647 (2010).
[16] Oxford Diffraction. *CrysAlis CCD and CrysAlis RED*, Versions 171.32.29, Oxford Diffraction Ltd., Abingdon, Oxfordshire, England (2008).
[17] G.M. Sheldrick. *Acta Crystallogr.*, **A64**, 112 (2008).
[18] A.L. Spek. *J. Appl. Crystallogr.*, **36**, 7 (2003).
[19] L.J. Farrugia. *J. Appl. Crystallogr.*, **30**, 565 (1997).
[20] C.F. Macrae, I.J. Bruno, J.A. Chisholm, P.R. Edgington, P. McCabe, E. Pidcock, L. Rodriguez-Monge, R. Taylor, J. van de Streek, P.A. Wood. *J. Appl. Crystallogr.*, **41**, 466 (2008).
[21] A. Cousson, F. Nectoux, F. Robert, E.N. Rizkalla. *Acta Crystallogr.*, **C51**, 838 (1995).
[22] G.B. Deacon, R.J. Philips. *Coord. Chem. Rev.*, **33**, 227 (1980).
[23] B.-M. Kukovec, Z. Popović, B. Kozlevčar, Z. Jagličić. *Polyhedron*, **27**, 3631 (2008).

[24] K. Nakamoto. *Infrared and Raman Spectra of Inorganic and Coordination Compounds*, 4th Edn, Wiley Interscience, New York (1986).
[25] H. Aghabozorg, E. Sadr-khanlou, A. Shokrollahi, M. Ghaedi, M. Shamsipur. *J. Iran. Chem. Soc.*, **6**, 55 (2009).
[26] Z. Aghajani, H. Aghabozorg, E. Sadr-khanlou, A. Shokrollahi, S. Derki, M. Shamsipur. *J. Iran. Chem. Soc.*, **6**, 373 (2009).
[27] A.D. Kulkarni, S.A. Patil, P.S. Badami. *Int. J. Electrochem. Sci.*, **4**, 717 (2009).
[28] A.J. Bard, L.R. Faulkner. *Fundamentals and Applications*, Wiley, New York (2001).
[29] Y. Zhou, Y. Ge, S. Gou, H. Ju, J. Liu. *Transition Met. Chem.*, **22**, 347 (1997).